Journal of Hepatocellular Carcinoma

Dovepress

open access to scientific and medical research

Open Access Full Text Article

ORIGINAL RESEARCH

An Oxidative Stress-Related Prognostic Signature Predicts Treatment Response and Outcomes for Hepatocellular Carcinoma After Transarterial Chemoembolization

Hui Ma[1,2]*, Ting Yu[3]*, Zhong-Chen Li[1], Lan Zhang[1,2], Rong-Xin Chen[1], Zheng-Gang Ren[1]

[1]Liver Cancer Institute, Zhongshan Hospital, Fudan University, Shanghai, People's Republic of China; [2]Department of Hepatic Oncology, Xiamen Branch, Zhongshan Hospital, Fudan University, Xiamen, People's Republic of China; [3]Department of Pathology, Obstetrics and Gynecology Hospital, Fudan University, Shanghai, People's Republic of China

*These authors contributed equally to this work

Correspondence: Hui Ma, Email mahui_676@163.com

Purpose: Oxidative stress plays a critical role in promoting tumor resistance to hypoxia and chemotherapeutic drugs. However, the prognostic role of oxidative stress-related genes (OSRGs) in hepatocellular carcinoma (HCC) treated with transarterial chemoembolization (TACE) has not been fully explored.

Methods: We used transcriptome data from the GSE104580 cohort containing patients marked as responders or nonresponders to TACE therapy to identify differentially expressed OSRGs associated with TACE response (TR-OSRGs). We created a TR-OSRG prognostic signature based on TR-OSRGs using least absolute shrinkage and selection operator Cox and stepwise Cox regression analyses in a training cohort of patients with HCC (TCGA-LIHC). We verified this prognostic signature in two external cohorts of patients who received TACE for HCC (GSE14520-TACE and ZS-TACE-37). Finally, we constructed a prognostic nomogram model for predicting survival probability of patients with HCC based on Cox regression analysis.

Results: The TR-OSRG prognostic signature was created and shown to be a robust independent prognostic factor for treatment response and outcomes for HCC after TACE therapy. Risk scores based on this signature correlated with tumor stage and grade. Tumor samples from patients with higher risk scores exhibited more infiltration of immune cells and significantly increased expression of immune checkpoint genes. We also developed a nomogram for patients with HCC based on the TR-OSRG prognostic signature and clinical parameters; this nomogram was a useful quantitative analysis tool for predicting patient survival.

Conclusion: The TR-OSRGs signature exhibited good performance in predicting treatment response and outcomes in patients with HCC treated with TACE.

Keywords: hepatocellular carcinoma, transarterial chemoembolization, oxidative stress, response, prognosis

Introduction

Globally, primary liver cancer is the sixth most common cancer and the fourth leading cause of cancer-related deaths.[1] Hepatocellular carcinoma (HCC) is the most common type of liver cancer and is usually diagnosed at an advanced stage, resulting in limited treatment options.[2]

Transcatheter arterial chemoembolization (TACE) is recommended as first-line treatment for patients with unresectable localized liver tumors and well-preserved liver function.[3] TACE therapy is an image-guided procedure in which drugs that slow or halt tumor development are injected into the artery supplying the HCC.[4] The goals are to induce tumor ischemia by blocking the blood supply and to enhance antitumoral chemotherapeutic effects via retention of chemotherapeutics within the tumor environment.[4] Currently, TACE has been shown to improve the median survival of patients to

Received: 23 February 2024
Accepted: 1 August 2024
Published: 13 August 2024

around 30 months for BCLC intermediate-stage HCC and up to 13 months when combined with sorafenib in patients with advanced-stage HCC.[5] However, TACE is ineffective for some patients, and performing TACE when inappropriate may cause harm and reduce overall survival.[6] Therefore, it is of utmost importance to improve the selection of patients with HCC who are most likely to benefit from TACE.

Genomic analyses have revealed substantial differences in the molecular characteristics of HCC cells and their tumor microenvironment, even in samples with the same clinical grade.[2] Variations in molecular typing among patients with HCC are also associated with differences in treatment efficacy and prognosis.[7] Increasing evidence suggests that oxidative stress contributes to HCC tumorigenesis and progression.[8] Oxidative stress results from an imbalance between reactive oxygen species (ROS) and antioxidant molecules in cells and ultimately leads to DNA, lipid, and protein damage.[9] HCC typically develops in the setting of chronic viral hepatitis (especially hepatitis B and hepatitis C), nonalcoholic steatohepatitis, and cirrhosis, disorders that may promote the production of ROS and induction of oxidative stress in tumor cells and their microenvironment.[10] Notably, chemoembolization-induced ischemia, hypoxia, and chemical injury can induce ROS production in tumor cells and their microenvironment, and the resulting oxidative stress may promote HCC cell resistance to hypoxia and chemotherapeutic drugs.[8,10,11] We thereby hypothesize that patient response and outcomes following TACE are related to the oxidative stress signature and that this signature may be utilized prospectively to predict prognosis.

In this study, we used a systematic and comprehensive integrative analysis of oxidative stress-related genes associated with response to TACE (TR-OSRGs) to construct and verify a prognostic signature for predicting treatment response and outcomes in patients with HCC treated with TACE. We analyzed the prognostic value of the signature and developed a prognostic nomogram based on the TR-OSRG signature to provide a quantitative analysis tool for predicting prognostic risk in patients with HCC.

Materials and Methods

Data Acquisition and Identification of TR-OSRGs

This study included mRNA expression data and clinical information of patients with HCC obtained from three publicly available datasets: The Cancer Genome Atlas Liver Hepatocellular Carcinoma data collection (TCGA-LIHC), as well as the GSE14520[12] and GSE104580 datasets from the Gene Expression Omnibus. From the GSE14520 development cohort, we selected 104 patients who received TACE therapy (the GSE14520-TACE cohort). The GSE104580 dataset contains data from 147 patients treated with TACE, 81 of whom responded well (TACE responders) and 66 of whom responded poorly (TACE nonresponders). Gene sets associated with oxidative stress were acquired from the Molecular Signatures Database[13] (http://www.gsea-msigdb.org/gsea/msigdb).

Human Hepatocellular Carcinoma Specimens

HCC specimens were obtained from a subset of patients in the ZS cohort. This cohort included 432 patients with HCC who developed recurrent tumors after undergoing surgical resection with curative intent at the Liver Cancer Institute and Zhongshan Hospital of Fudan University between January 2014 and December 2015. Use of these specimens entailed patient informed consent and approval of our institutional Ethics Review Committee.

For this study, we included 37 patients who developed HCC recurrence within 1 year after surgery (the ZS-TACE-37 cohort). All patients in the ZS-TACE-37 cohort received a combination of chemotherapeutic agents, such as 5-fluorouracil, oxaliplatin, and lipiodol, during their TACE procedure. Modified Response Evaluation Criteria in Solid Tumors was used to assess response to TACE.[14] A complete or partial response was defined as a response. Progressive or stable disease was defined as a nonresponse.

Immunohistochemistry (IHC)

Pathology slides were stained according to standard procedures. Briefly, after overnight incubation with primary antibody at 4°C, the slides were incubated with the appropriate secondary antibodies. Images were obtained under light microscopy, with three randomly selected fields used for uniform image capture. Staining intensity (0, 1+, 2+, or 3+) was determined for each cell in a fixed field, and an H-score was assigned using this formula: $\mathrm{H-score} = 1\times(\%\ \mathrm{of}\ 1+\mathrm{cells}) + 2\times(\%\ \mathrm{of}\ 2+\mathrm{cells}) + 3\times(\%\ \mathrm{of}\ 3+\mathrm{cells})$.[15]

Nonnegative Matrix Factorization Clustering Algorithm

The R package limma[16] (version 3.10.3, http://www.bioconductor.org/packages/2.9/bioc/html/limma.html) was used to analyze differentially expressed genes (DEGs) between the TACE responder and nonresponder groups in the GSE104580 dataset. An absolute log2 fold change value >0.585 and an adjusted p value <0.05 were used to identify DEGs, from which differentially expressed OSRGs were extracted. KEGG analysis of the DEGs was performed using the R package clusterProfiler (version 4.4.4, http://bioconductor.org/packages/release/bioc/html/clusterProfiler.html). HCC samples from TCGA-LIHC were grouped using the R package ConsensusClusterPlus[17] (version 1.54.0, http://www.bioconductor.org/packages/release/bioc/html/ConsensusClusterPlus.html). The number of clusters (K) ranged from 2 to 6, and cophenetic, dispersion, and profile measures were used to determine the ideal number of clusters.

Establishment of a Protein-Protein Interaction (PPI) Network

We explored possible interactions between proteins using data from the Search Tool for the Retrieval of Interacting Genes/Proteins[18] (STRING, version 11.5, http://string-db.org/), with the interaction score 0.4.

Construction and Validation of the TR-OSRG Prognostic Signature

Univariate Cox regression analysis was performed to identify prognosis-related DEGs in the TCGA-LIHC dataset using the R package gwasurvivr (version 1.16.0, https://bioconductor.org/packages/gwasurvivr/). Least absolute shrinkage and selection operator (LASSO) Cox and stepwise Cox regression analyses were performed to evaluate key prognosis-related qualities and to establish prognostic characteristics using the R package glmnet (version 1.2, https://cran.r-project.org/web/packages/glmnet/index.html) and survminer (version 0.4.9, https://cran.rstudio.com/web/packages/survminer/index.html). A risk score (RS) was created based on gene expression levels and corresponding coefficient values. Specifically, we first standardize gene expression levels across all patient samples to ensure comparability. Next, using LASSO Cox regression analysis, we determine regression coefficients (weights) for each gene in the prognostic model. Finally, we calculate the RS by multiplying the standardized expression value of each gene by its respective regression coefficient and summing these products to derive the overall RS. Subsequently, we stratified patients into two subgroups according to the median RS. The ability of the prognostic signature to predict survival and estimate risk was evaluated by receiver operating characteristic (ROC) curves, Kaplan–Meier survival analysis, and Cox models of relative risk.[19]

Assessment of Immune Cell Infiltration

We used the MCP counter[20] (http://github.com/ebecht/MCPcounter) to quantify the subsets of infiltrating immune cells in the tumor environment of HCC samples. The Immune score and Stromal score of tumor tissues were determined using the R package ESTIMATE (https://bioinformatics.mdanderson.org/estimate/rpackage.html). Correlations between *PDGFD, G6PD*, and *ADAM9* expression and expression of immune checkpoint genes in human HCC tissues were estimated using Tumor Immune Evaluation Resource[21] (TIMER, https://cistrome.shinyapps.io/timer/). Correlations between *PDGFD, G6PD*, and *ADAM9* expression and infiltration scores of immune cells (CD4+ T cells, CD8+ T cells, macrophages, and dendritic cells) in human HCC tissues were also estimated using TIMER.

Construction of a Prognostic Nomogram

Univariate and multivariate Cox regression analyses were used to identify independent prognostic characteristics of patients with HCC in the TCGA-LIHC cohort. The regression analysis results were then used to construct a prognostic nomogram model for predicting survival probability of patients with HCC. R package rms (version 5.1–2, https://cran.r-project.org/web/packages/rms/index.html) was used to generate a calibration graph showing the differences between predicted and actual survival rates of patients with HCC.

Statistical Analysis

All statistical analyses were performed with R software (version 4.0.3) or GraphPad Prism (version 7.0), setting the level of statistical significance at $p<0.05$. Unpaired Student's *t*-tests, Pearson χ^2 tests, or Fisher's exact tests were used for comparisons, as appropriate. Correlations were evaluated using Pearson's *r*. For Kaplan–Meier survival curves, statistical significance was estimated using the Log rank test.

Results

Identification of Hepatocellular Carcinoma Clusters Based on TR-OSRGs

By analyzing differences in gene expression between 81 TACE responders and 66 TACE nonresponders in GSE104580, we identified 45 differentially expressed TR-OSRGs. Based on these genes, we created a heat induction map (Figure 1A). We then performed KEGG enrichment analysis on these TR-OSRGs and found that tumorigenesis and immunomodulatory pathways were significantly enriched (Figure 1B). Based on TR-OSRG expression, patients with HCC in TCGA-LIHC were classified into two groups (cluster 1 and cluster 2) using the NMF clustering algorithm (Figure 1C). The Immune score, Stromal score, and ESTIMATE score were significantly higher in cluster 2 than in cluster 1 ($p<0.0001$,

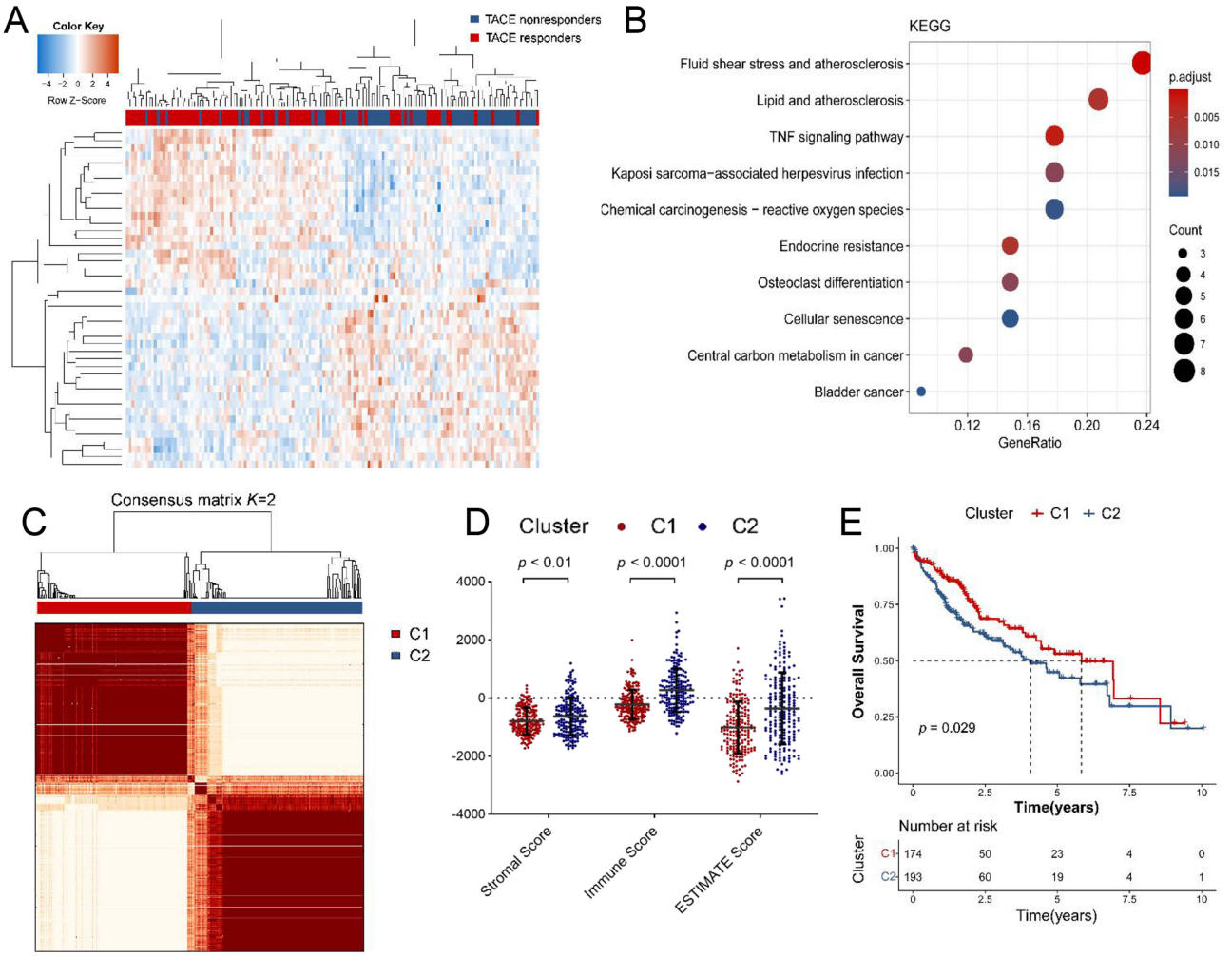

Figure 1 Identification of hepatocellular carcinoma clusters based on TR-OSRGs. (**A**) Heatmap showing the expression profiles of 45 differentially expressed TR-OSRGs identified from the comparison between 81 TACE responders and 66 TACE nonresponders in GSE104580. (**B**) KEGG enrichment analysis of 45 differentially expressed TR-OSRGs. (**C**) Heatmap of HCC subtypes based on TR-OSRGs using the NMF clustering algorithm (*K*=2), showing the classification of TCGA-LIHC patients into two subgroups (cluster 1 and cluster 2). (**D**) Comparison of Stromal score and Immune score between the two HCC subtypes using ESTIMATE algorithm. (**E**) Kaplan-Meier curve of overall survival for two HCC subtypes, with significantly worse survival outcomes observed in cluster 2 compared to cluster 1. TR-OSRGs, oxidative stress-related genes associated with transarterial chemoembolization response.

$p<0.01$, and $p<0.0001$, respectively, Figure 1D), and overall survival was significantly worse in cluster 2 than in cluster 1 ($p=0.029$, Figure 1E).

Construction of the TR-OSRG Prognostic Signature

We identified 28 prognosis-related TR-OSRGs in the TCGA-LIHC cohort using univariate Cox regression analysis and generated a correlation matrix by performing correlation analysis (Figure 2A). The PPI of these 28 molecules is shown in Figure 2B. We then constructed a prognostic prediction model based on the prognosis-related TR-OSRGs using LASSO Cox regression analysis (Figure 2C and D). Using stepwise Cox regression methodology, we generated an RS representing the oxidative stress status for the TR-OSRG signature based on the expression levels of three genes and their corresponding coefficients: RS = –0.1655 × *PDGFD* + 0.2184 × *G6PD* + 0.2398 × *ADAM9*. A forest plot showed that these three genes were closely associated with prognosis (Figure 2E). The GSE104580 nonresponder group had a significantly higher RS, with lower *PDGFD*, higher *G6PD*, and higher *ADAM9* expression levels, compared to the responder group (Figure 2F and G). RS was calculated for each patient in the TCGA-LIHC cohort, and patients were divided into high- and low-risk groups based on the median RS. A scatter plot was created to depict the distribution of RS and their association with survival (Figure 2H). Kaplan–Meier survival analysis revealed that patients with a high RS had a worse prognosis, and ROC analysis showed that the TR-OSRG signature had good prognostic performance, with area under the curve (AUC) values of 0.744, 0.684, and 0.605 at 1-, 3-, and 5-year, respectively (Figure 2H).

Validation of the TR-OSRG Prognostic Signature

To further assess the predictive ability of the TR-OSRG signature for estimating the prognosis of patients with HCC who received TACE, external validation was performed using the GSE14520-TACE cohort. The RS was calculated for each patient using the same formula as above, and patients were classified into high- and low-risk groups according to the median RS in this validation cohort. The distribution of RS values and their associations with survival are illustrated in Figure 3A. Kaplan–Meier survival and ROC analyses were performed. Patients in the high-risk group had shorter overall survival than those in the low-risk group, and the AUCs of the TR-OSRG signature for 1-, 3-, and 5-year survival are shown in Figure 3A.

We also performed immunohistochemistry to evaluate expression levels of the three TR-OSRGs in the ZS-TACE-37 cohort. This cohort included 15 patients who were TACE responders and 22 patients who were TACE nonresponders. The H-score was calculated to quantify the expression of each protein. Statistical analysis revealed that the nonresponder group had lower PDGFD, higher G6PD, and higher ADAM9 expression levels than the responder group (Figure 3B and C). The RS based on the H-score was then calculated for each patient in the ZS-TACE-37 cohort, and the nonresponder group was found to have a significantly increased RS, compared with the responder group (Figure 3D). Patients were divided into high- and low-RS groups according to the median RS, and survival analysis revealed that the high-RS group had an inferior prognosis, consistent with the prognostic role of mRNA levels (Figure 3E). These results thus indicate that the TR-OSRG prognostic signature was successfully verified in external cohorts of patients with HCC treated with TACE.

Construction of a Nomogram Based on the TR-OSRG Prognostic Signature

To assess the independence of the TR-OSRG prognostic signature for clinical applications, we performed Cox regression analysis in the TCGA-LIHC cohort. Significant correlations between RS and prognosis were found during both univariate regression analysis (hazard ratio [95% CI] = 1.753 [1.238–2.484], $p=0.002$) (Figure 4A) and multivariate regression analysis (hazard ratio [95% CI] = 1.717 [1.169–2.522], $p=0.006$) (Figure 4B), suggesting that the TR-OSRG prognostic signature had good independent clinical predictive value. Multiple regression revealed only two variables with a p value <0.05—tumor stage and RS—and a nomogram model was established to predict the survival risk of patients with HCC (Figure 4C). As shown in Figure 4D, there was good agreement between the predicted and actual 1-, 3-, and 5-year survival rates, as indicated by the amount of overlap between calibration curves. Moreover, HCC samples with a high nomogram score were associated with a significantly worse prognosis than those with a low nomogram score (Figure 4E). The AUC values of the prognostic model were 0.767, 0.739, and 0.698 for 1-, 3-, and 5-year survival, respectively (Figure 4F), thereby confirming the good prognostic value of our model.

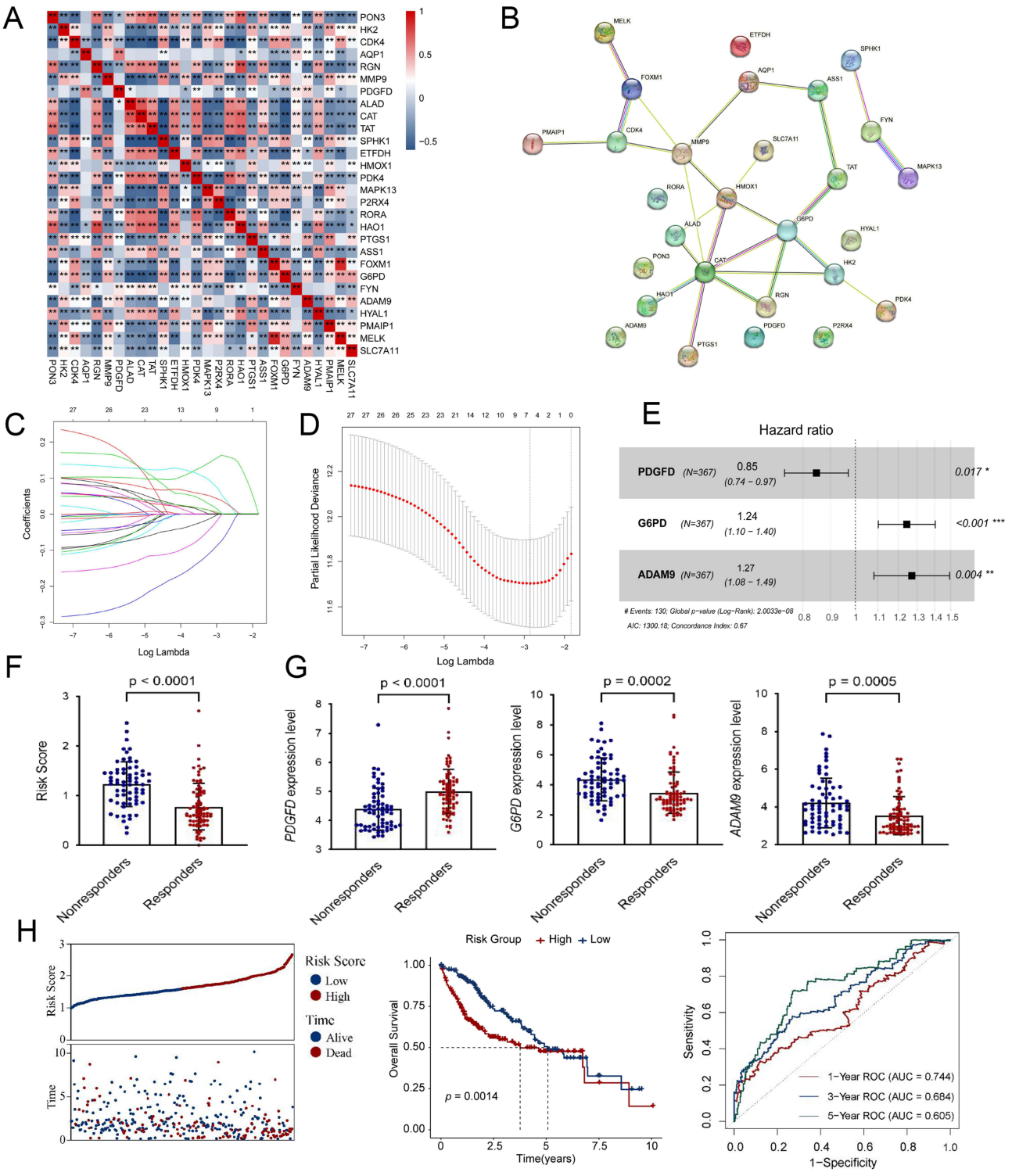

Figure 2 Construction of the TR-OSRG prognostic signature. (**A**) The correlation heatmap of 28 prognosis-related TR-OSRGs in the TCGA-LIHC cohort. (**B**) A PPI of the 28 prognosis-related TR-OSRGs was plotted using STRING. (**C**) Coefficients of independent variables in LASSO regression. (**D**) Cross-validation of parameter selection in LASSO regression. (**E**) Forest plot of the TR-OSRG model by stepwise Cox regression algorithm, illustrating the prognostic associations of PDGFD, G6PD, and ADAM9. (**F**) RS calculated using the TR-OSRG signature, with a higher RS in nonresponders compared to responders in the GSE104580 cohort. (**G**) Expression levels of PDGFD, G6PD, and ADAM9. (**H**) Distribution of risk scores and survival status in the internal (TCGA-LIHC) cohort; Kaplan-Meier curve analyses for the high-risk and low-risk groups in the internal cohort, and the ROC curves of the TR-OSRG prognostic signature at 1, 3, and 5 years in the internal cohort.

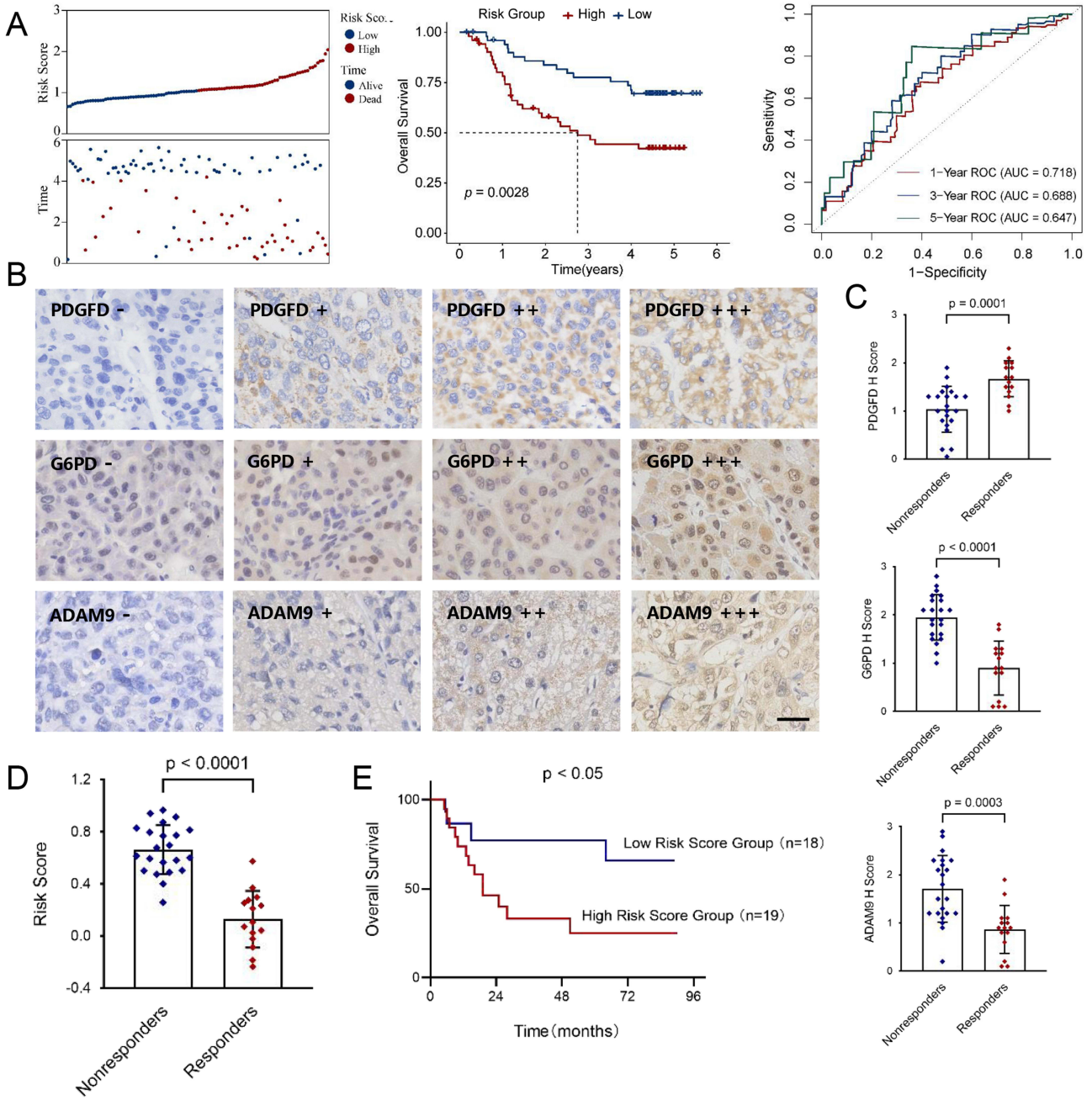

Figure 3 Validation of the TR-OSRG prognostic signature. (**A**) Distribution of risk scores and survival status in the external (GSE14520-TACE) cohort; Kaplan-Meier curve analyses for the high-risk and low-risk groups in the external cohort, and the ROC curves of the TR-OSRG prognostic signature at 1, 3, and 5 years in the external cohort. (**B**) Representative immunohistochemistry staining images of PDGFD, G6PD and ADAM9 in the ZS-TACE-37 cohort (scale bar, 25 μm). The difference in the H-score of 3 model-related TR-OSRG proteins (**C**) Differences in H-scores for PDGFD, G6PD, and ADAM9 between TACE responders and nonresponders in the ZS-TACE-37 cohort. (**D**) RS based on H-scores for the TR-OSRG model, with significantly higher RS in the nonresponder group compared to responders. (**E**) Kaplan-Meier curve analyses for the high-risk and low-risk groups in the ZS-TACE-37 cohort.

Correlation of the TR-OSRG Prognostic Signature with Clinical Features and Immune Cell Infiltration

To investigate whether the TR-OSRG prognostic signature correlated with clinical features and response to immunotherapy, we compared the RS of different subgroups in the TCGA-LIHC cohort. The RS was lower in cluster 1 (with a better prognosis) than in cluster 2 (Figure 5A), and the RS was higher in HCC samples from advanced-stage tumors than in samples from early-stage HCC (Figure 5B and C). HCC samples with higher tumor pathologic grade had a significantly

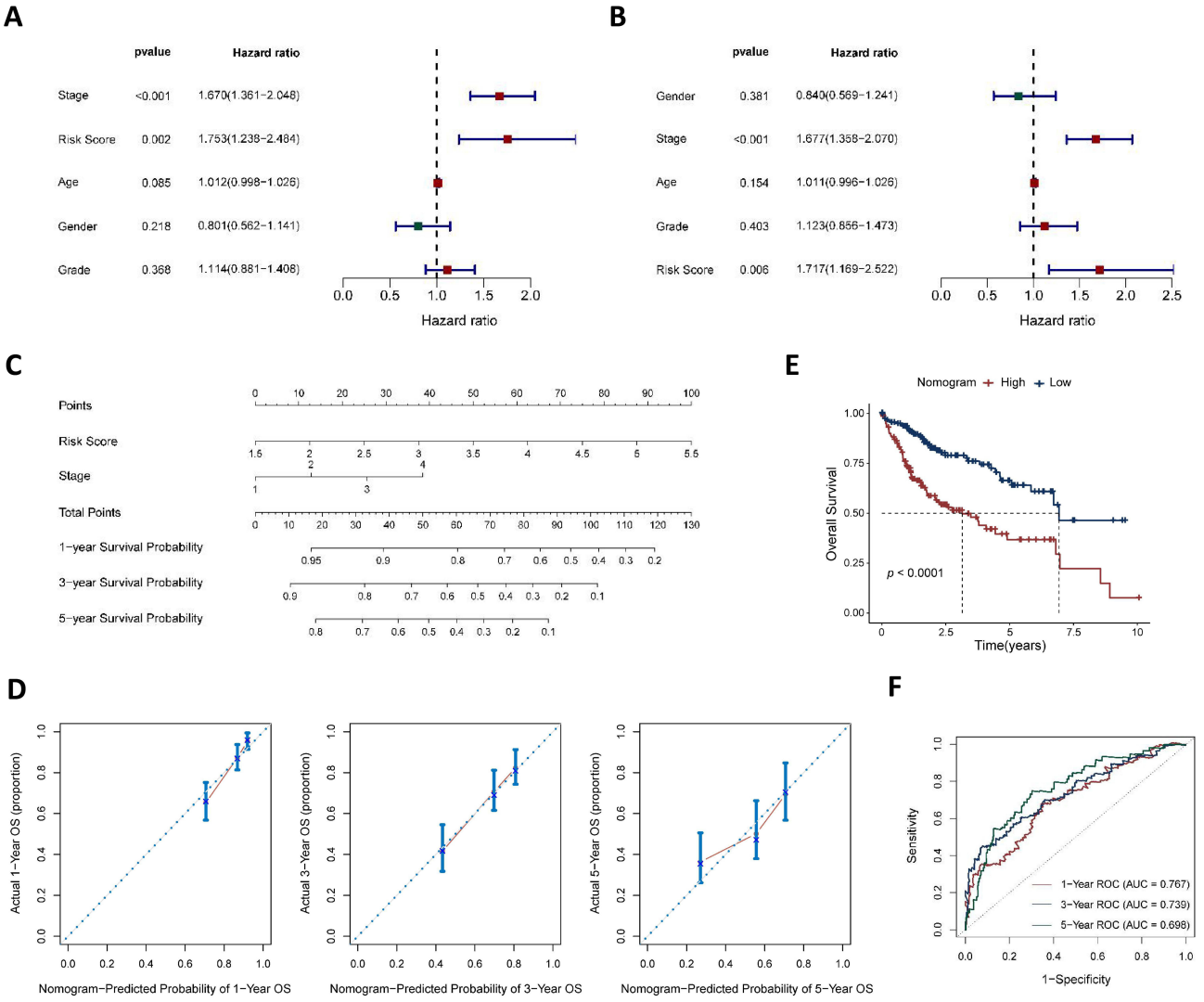

Figure 4 Construction of a nomogram based on the TR-OSRG prognostic signature. (**A**) Univariate Cox regression and (**B**) multivariate Cox regression analyses of the TR-OSRG prognostic signature in the TCGA-LIHC cohort. (**C**) Nomogram for predicting the overall survival in TCGA-LIHC cohort at 1, 3, and 5 years. (**D**) Calibration curve for consistency between 1-year, 3-year, and 5-year nomogram-predicted survival and actual survival. (**E**) Kaplan-Meier curve of overall survival for high and low nomogram score groups. (**F**) ROC curves of nomograms for 1-year, 3-year, and 5-year survival.

higher RS (Figure 5D). To further understand the effect of the TR-OSRG prognostic signature on immunotherapy efficacy, correlations between RS and immune cell infiltration were analyzed. As shown in Figure 5E, tumors from the high-RS group exhibited more infiltration of T cells, CD8+ T cells, B cells, monocytes (macrophages), and dendritic cells, compared with tumors from the low-RS group. The higher T cell (CD3) and macrophage (CD68) infiltration in the high-RS group was also verified in the ZS-TACE-37 cohort (Figure 5F and G). Given the association between higher RS and tumor immunosuppression, the correlation between RS and expression of common immune checkpoint genes was also investigated. Interestingly, the high-RS group had significantly increased immune checkpoint gene expression (Figure 5H). Among the three genes in the risk model, *G6PD* was the gene most closely correlated with the expression of these immune checkpoint genes (Figure 5I). In total, our findings indicate that the TR-OSRG signature has good prognostic predictive power, in accordance with differences in clinical characteristics and immune cell infiltration between tumors.

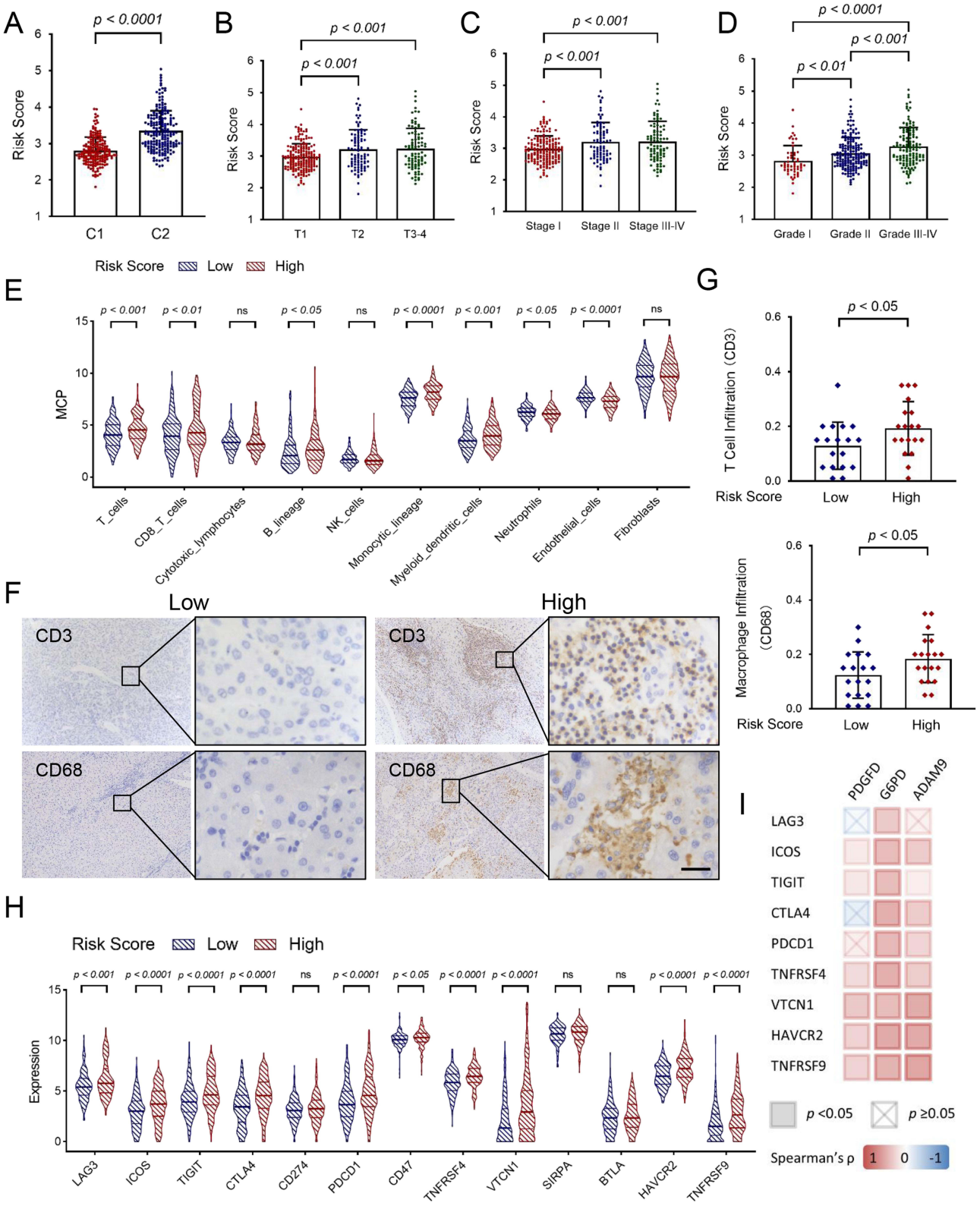

Figure 5 Correlation of the TR-OSRG prognostic signature with clinical features and immune cell infiltration. The difference in risk scores between different clinical features of (**A**) cluster molecular subtype, (**B** and **C**) tumor stage, and (**D**) tumor grade in the TCGA-LIHC cohort. (**E**) Comparison of the difference in immune cell infiltration between the high-risk and low-risk groups in the TCGA-LIHC cohort. (**F**) Representative immunohistochemistry staining images showing low expression (left) and high expression (right) of CD3 and CD68 are shown (scale bar, 25 μm). (**G**) Comparison of the difference in T cell and macrophage infiltration between the high-risk and low-risk groups in the ZS-TACE-37 cohort. (**H**) Comparison of the difference in common immune checkpoint genes expression between the high-risk and low-risk groups in the TCGA-LIHC cohort. (**I**) Correlation analysis between *PDGFD, G6PD* and *ADAM9* expression and common immune checkpoint genes expression in human HCC tissues estimated by TIMER (Spearman's ρ>0, positive correlation; Spearman's ρ<0, negative correlation).

Discussion

HCC is a common digestive system tumor with high aggressiveness and a poor prognosis.[2] In the current era of precision medicine, in which predictive and prognostic biomarkers guide treatment based on molecular tumor features, advances in HCC treatment have lagged behind that of other tumors.[22] TACE is currently a standard treatment for patients with unresectable HCC, especially those with BCLC intermediate-stage disease.[3] As increasing attention focuses on the response to TACE therapy, there is an urgent need to detect gene signatures or biomarkers specifically associated with prognosis after TACE to aid in the identification of patients most likely to benefit from this treatment.

Different ROS control diverse aspects of tumor cell behavior from signaling to death, and deregulation of ROS production and ROS limitation pathways are features of HCC cells and their microenvironment.[8] ROS also modulate the tumor environment, affecting the various stromal cells providing metabolic support, blood supply, and immune responses to the tumor.[8] The oxidative stress state of tumor tissues, therefore, may affect the response to TACE therapy in patients with HCC, a treatment based on embolization of tumor blood supply and chemotherapy injury of tumor cells.[4]

In this study, we identified OSRGs differentially expressed between TACE responders and nonresponders (ie, TR-OSRGs) based on the GSE104580 dataset. We then used LASSO Cox and stepwise Cox regression analyses in the training cohort TCGA-LIHC to construct a TR-OSRG prognosis signature for HCC consisting of *PDGFD, G6PD*, and *ADAM9* and successfully verified the validity of this signature in two external cohorts: GSE14520-TACE and ZS-TACE -37. We subsequently developed a nomogram based on the TR-OSRG prognostic signature and clinical parameters for patients with HCC, which was found to be an effective quantitative analysis tool for predicting patient survival. RSs based on the TR-OSRG prognostic signature correlated with tumor stage and grade; higher RS values were associated with greater infiltration of immune cells (eg, T cells, CD8+ T cells, B cells, monocytes [macrophages], dendritic cells) and significantly increased expression of immune checkpoint genes.

Platelet-derived growth factor D (PDGFD) is a member of the PDGF family of proteins. It is involved in the pathogenesis and progression of human cancer by regulating cell proliferation, apoptosis, migration, invasion, angiogenesis, and metastasis.[23] PDGFD is significantly upregulated by oxidative stress and has been demonstrated to increase macrophage recruitment, interstitial fluid pressure, and maturation of blood vessels during angiogenesis.[24] Glucose-6-phosphate dehydrogenase (G6PD) is the first and rate-limiting enzyme of the oxidative branch of the pentose phosphate pathway. G6PD has antioxidant properties and plays a major role in the anabolic metabolism of ribose 5-phosphate for nucleotide synthesis, regeneration of the reduced form of nicotinamide adenine dinucleotide phosphate (NADPH) for reductive lipid biosynthesis, and regeneration of glutathione for detoxification of ROS.[25] It also has a prooxidant role in generating ROS via NADPH oxidase.[25] Aberrant activation of G6PD via metabolic reprogramming alters NADPH levels, leading to an antioxidant or a prooxidant environment that may contribute to cancer development and resistance to therapies.[26] A disintegrin and metalloprotease (ADAM) is a modular type I transmembrane protein that contains a metalloprotease domain and a disintegrin-like domain. ADAM9 possesses potent biologic activities; is highly expressed in cancers of the liver, prostate, pancreas, breast, and colon; and is associated with cancer progression and poor clinical outcomes.[27] When tumor cells are subjected to crowding and hypoxic stress conditions, ADAM9 expression is upregulated, which is mediated through ROS.[28] Upregulation of ADAM9 could facilitate cancer development, promote cancer cell invasion and migration, and increase resistance to stress-induced injuries.[29]

Induction of ischemia and hypoxia by hepatic artery occlusion and induction of tumor cell injury by introducing chemotherapeutic agents are the key components of TACE for HCC and lead to altered oxidative stress status.[5] In tumors from patients who fail to respond to TACE, it is possible that the tumor microenvironment has undergone reprogramming of oxidative stress-related pathways prior to treatment, as evidenced by differential expression of TR-OSRGs. However, the precise mechanism of TACE resistance remains unclear. In recent years, oxidative stress has been associated with tumor immune microenvironment remodeling.[30] Oxidative stress can cause oxidative DNA damage, which is an important initiator of malignant tumors.[31] Persistent oxidative DNA damage can remodel the HCC microenvironment through the cyclic GMP-AMP synthase and stimulator of interferon genes (cGAS-STING) pathway, leading to recruitment of macrophages and T lymphocytes within the tumors, promoting the expression of immune checkpoint proteins, and creating an immunosuppressive tumor microenvironment.[32] In addition, persistently elevated ROS levels can affect

immune cell function by regulating cellular metabolism and further aggravate immune cell exhaustion.[8] These findings provide a mechanistic explanation for our results. However, further investigations are required to determine the specific mechanisms underlying the effects of cross-talk between oxidative stress and immune microenvironment remodeling on the response to TACE in patients with HCC.

This study has some limitations. First, the development of a predictive tool using retrospective data to help select patients suitable for TACE treatment is only the first milestone. Conducting prospective clinical trials in different populations is a critical future direction. Second, changes in the expression of the studied genes before and after TACE treatment were not considered. Lastly, we did not provide the overall survival and progression-free survival rates of TACE responders and non responders. This limitation affected the comprehensiveness of our findings. Future research should include long-term follow-up data to validate the prognostic signature and enhance the robustness of survival analyses. Conducting studies with extended follow-up periods and larger patient populations will help address these shortcomings and further solidify our conclusions.

Conclusion

We created a novel prognostic signature based on an integrated analysis of TR-OSRGs. This signature has satisfactory performance for predicting treatment response and outcomes in patients with HCC treated with TACE. We also used this signature to develop a nomogram for patients with HCC receiving TACE therapy. This nomogram is an effective quantitative analysis tool for the clinical application of personalized precision therapy.

Data Sharing Statement

Publicly available datasets were analyzed in this study, and the names of the repositories can be found in the article. Additional data supporting the findings of this study are available from the corresponding author upon request.

Ethics Statement

The study involving human participants was reviewed and approved by the Ethics Review Committee of Zhongshan Hospital of Fudan University (permission number B2024-105). This study followed the Declaration of Helsinki (2013 revision).

Acknowledgments

Hui Ma and Ting Yu are co-first authors for this study. We thank all participants in the TCGA-LIHC, GSE14520, GSE104580, and ZS-TACE-37 cohorts.

Funding

This research project was supported in part by a grant from The National Natural Science Foundation of China (81502010) and The Shanghai Pujiang Program (23PJ1401300).

Disclosure

The authors report no conflicts of interest in this work.

References

1. Sung H, Ferlay J, Siegel RL, et al. Global cancer statistics 2020: GLOBOCAN estimates of incidence and mortality worldwide for 36 cancers in 185 countries. *CA Cancer J Clin*. 2021;71(3):209–249. doi:10.3322/caac.21660
2. Llovet JM, Kelley RK, Villanueva A, et al. Hepatocellular carcinoma. *Nat Rev Dis Primers*. 2021;7(1):6. doi:10.1038/s41572-020-00240-3
3. Singal AG, Kudo M, Bruix J. Breakthroughs in hepatocellular carcinoma therapies. *Clin Gastroenterol Hepatol*. 2023;21(8):2135–2149. doi:10.1016/j.cgh.2023.01.039
4. Chang Y, Jeong SW, Young Jang J, Jae Kim Y. Recent updates of transarterial chemoembolilzation in hepatocellular carcinoma. *Int J Mol Sci*. 2020;21(21):8165. doi:10.3390/ijms21218165
5. Zhong BY, Jin ZC, Chen JJ, Zhu HD, Zhu XL. Role of transarterial chemoembolization in the treatment of hepatocellular carcinoma. *J Clin Transl Hepatol*. 2023;11(2):480–489. doi:10.14218/JCTH.2022.00293

6. Kotsifa E, Vergadis C, Vailas M, et al. Transarterial chemoembolization for hepatocellular carcinoma: Why, When, How? *J Pers Med*. 2022;12(3):436. doi:10.3390/jpm12030436
7. Zhu AX, Abbas AR, de Galarreta MR, et al. Molecular correlates of clinical response and resistance to atezolizumab in combination with bevacizumab in advanced hepatocellular carcinoma. *Nat Med*. 2022;28(8):1599–1611. doi:10.1038/s41591-022-01868-2
8. Cheung EC, Vousden KH. The role of ROS in tumour development and progression. *Nat Rev Cancer*. 2022;22(5):280–297. doi:10.1038/s41568-021-00435-0
9. Holmstrom KM, Finkel T. Cellular mechanisms and physiological consequences of redox-dependent signalling. *Nat Rev Mol Cell Biol*. 2014;15(6):411–421. doi:10.1038/nrm3801
10. Uchida D, Takaki A, Oyama A, et al. Oxidative stress management in chronic liver diseases and hepatocellular carcinoma. *Nutrients*. 2020;12(6):1576. doi:10.3390/nu12061576
11. Tang P, Qu W, Wang T, et al. Identifying a hypoxia-related long non-coding RNAs signature to improve the prediction of prognosis and immunotherapy response in hepatocellular carcinoma. *Front Genet*. 2021;12:785185. doi:10.3389/fgene.2021.785185
12. Roessler S, Jia HL, Budhu A, et al. A unique metastasis gene signature enables prediction of tumor relapse in early-stage hepatocellular carcinoma patients. *Cancer Res*. 2010;70(24):10202–10212. doi:10.1158/0008-5472.CAN-10-2607
13. Subramanian A, Tamayo P, Mootha VK, et al. Gene set enrichment analysis: a knowledge-based approach for interpreting genome-wide expression profiles. *Proc Natl Acad Sci U S A*. 2005;102(43):15545–15550. doi:10.1073/pnas.0506580102
14. Lencioni R, Llovet JM. Modified RECIST (mRECIST) assessment for hepatocellular carcinoma. *Semin Liver Dis*. 2010;30(1):52–60. doi:10.1055/s-0030-1247132
15. John T, Liu G, Tsao MS. Overview of molecular testing in non-small-cell lung cancer: mutational analysis, gene copy number, protein expression and other biomarkers of EGFR for the prediction of response to tyrosine kinase inhibitors. *Oncogene*. 2009;28(Suppl 1):S14–S23.
16. Ritchie ME, Phipson B, Wu D, et al. limma powers differential expression analyses for RNA-sequencing and microarray studies. *Nucleic Acids Res*. 2015;43(7):e47. doi:10.1093/nar/gkv007
17. Wilkerson MD, Hayes DN. ConsensusClusterPlus: a class discovery tool with confidence assessments and item tracking. *Bioinformatics*. 2010;26(12):1572–1573. doi:10.1093/bioinformatics/btq170
18. Szklarczyk D, Gable AL, Nastou KC, et al. The STRING database in 2021: customizable protein-protein networks, and functional characterization of user-uploaded gene/measurement sets. *Nucleic Acids Res*. 2021;49(D1):D605–D612. doi:10.1093/nar/gkaa1074
19. Ma H, Li Z, Chen R, Ren Z. Development of a combined oxidative stress and endoplasmic reticulum stress-related prognostic signature for hepatocellular carcinoma. Comb Chem High Throughput Screen; 2024 27 19 2850–2860 doi:10.2174/0113862073257308231026073951.
20. Becht E, Giraldo NA, Lacroix L, et al. Estimating the population abundance of tissue-infiltrating immune and stromal cell populations using gene expression. *Genome Biol*. 2016;17(1):218. doi:10.1186/s13059-016-1070-5
21. Li T, Fan J, Wang B, et al. TIMER: a web server for comprehensive analysis of tumor-infiltrating immune cells. *Cancer Res*. 2017;77(21):e108–e110. doi:10.1158/0008-5472.CAN-17-0307
22. Fako V, Martin SP, Pomyen Y, et al. Gene signature predictive of hepatocellular carcinoma patient response to transarterial chemoembolization. *Int J Biol Sci*. 2019;15(12):2654–2663. doi:10.7150/ijbs.39534
23. Zou X, Tang XY, Qu ZY, et al. Targeting the PDGF/PDGFR signaling pathway for cancer therapy: a review. *Int J Biol Macromol*. 2022;202:539–557. doi:10.1016/j.ijbiomac.2022.01.113
24. Liu MY, Eyries M, Zhang C, Santiago FS, Khachigian LM. Inducible platelet-derived growth factor D-chain expression by angiotensin II and hydrogen peroxide involves transcriptional regulation by Ets-1 and Sp1. *Blood*. 2006;107(6):2322–2329. doi:10.1182/blood-2005-06-2377
25. Yang HC, Stern A, Chiu DT. G6PD: a hub for metabolic reprogramming and redox signaling in cancer. *Biomed J*. 2021;44(3):285–292. doi:10.1016/j.bj.2020.08.001
26. Yang HC, Wu YH, Yen WC, et al. The redox role of G6PD in cell growth, cell death, and cancer. *Cells*. 2019;8(9):1055. doi:10.3390/cells8091055
27. Chou CW, Huang YK, Kuo TT, Liu JP, Sher YP. An overview of ADAM9: structure, activation, and regulation in human diseases. *Int J Mol Sci*. 2020;21(20):7790. doi:10.3390/ijms21207790
28. Sung SY, Kubo H, Shigemura K, et al. Oxidative stress induces ADAM9 protein expression in human prostate cancer cells. *Cancer Res*. 2006;66(19):9519–9526. doi:10.1158/0008-5472.CAN-05-4375
29. Dong Y, Wu Z, He M, et al. ADAM9 mediates the interleukin-6-induced Epithelial-Mesenchymal transition and metastasis through ROS production in hepatoma cells. *Cancer Lett*. 2018;421:1–14. doi:10.1016/j.canlet.2018.02.010
30. Aboelella NS, Brandle C, Kim T, Ding ZC, Zhou G. Oxidative Stress in the Tumor Microenvironment and Its Relevance to Cancer Immunotherapy. *Cancers*. 2021;13(5):986. doi:10.3390/cancers13050986
31. Srinivas US, Tan BWQ, Vellayappan BA, Jeyasekharan AD. ROS and the DNA damage response in cancer. *Redox Biol*. 2019;25:101084. doi:10.1016/j.redox.2018.101084
32. Ma H, Kang Z, Foo TK, Shen Z, Xia B. Disrupted BRCA1-PALB2 interaction induces tumor immunosuppression and T-lymphocyte infiltration in HCC through cGAS-STING pathway. *Hepatology*. 2023;77(1):33–47. doi:10.1002/hep.32335